

Formation and evolution properties of clusters in liquid metal copper during rapid cooling processes

YI Xue-hua(易学华)^{1,2}, LIU Rang-su(刘让苏)¹, TIAN Ze-an(田泽安)¹,
HOU Zhao-yang(侯兆阳)¹, LI Xiao-yang(李晓阳)¹, ZHOU Qun-yi(周群益)¹

1. Department of Physics, Hunan University, Changsha 410082, China;

2. Department of Physics, Jiaying University, Meizhou 514015, China

Received 5 March 2007; accepted 23 July 2007

Abstract: Based on the quantum Sutton-Chen many-body potential, a molecular dynamics simulation was performed to investigate the formation and evolution properties of clusters in liquid Cu with 50 000 atoms. The cluster-type index method(CTIM) was used to describe the complex microstructure transitions. It is demonstrated that the amorphous structures are mainly formed with the three bond-types of 1551, 1541 and 1431 in the system, and the icosahedral cluster (12 0 12 0) and other basic polyhedron clusters of (12 2 8 2), (13 1 10 2), (13 3 6 4), (14 1 10 3), (14 2 8 4) and (14 3 6 5) play a critical and leading role in the transition from liquid to glass. The nano-clusters formed in the system consist of some basic clusters and middle cluster configurations by connecting to each other, and distinguish from those obtained by gaseous deposition and ionic spray. From the results of structural parameter pair distribution function $g(r)$, bond-types and basic cluster-types, it is found that the glass transition temperature T_g for liquid metal Cu is about 673 K at the cooling rate of 1.0×10^{14} K/s.

Key words: liquid metal Cu; microstructure transition; nano-cluster; molecular dynamics simulation; QSC many-body potential

1 Introduction

It is well known that it is difficult to obtain the microstructure evolution information in solidification processes of liquid metals under present experimental conditions. However, with the rapid development of computer technique, some important informations of microstructure evolution during solidification processes of liquid metals have been obtained by using molecular dynamics simulation[1–6]. In recent years, for the liquid metal Cu, the molecular dynamics simulation studies have been performed by using some well known model potentials, such as EAM[2, 5, 7], FS [8] and TB[9] potentials, to study the properties of microstructure transition of liquid metal Cu during rapid solidification processes and some important results have been obtained [5–9]. These results, however, from the view point of comprehensive understanding of the structures and properties of liquid Cu, are complementary each other.

To further investigate the microstructure evolution mechanism during solidification processes of liquid Cu, on the basis of previous works[4,10], a tracking

simulation study on the formation process of nano-clusters in a larger system consisting of 50 000 Cu atoms was devoted by adopting the quantum Sutton-Chen many-body potential and molecular dynamics method in this work. Using the cluster-type index method(CTIM) and the centre-atom method[4], the complex microstructure transitions were well described and analyzed.

2 Simulation conditions and methods

The conditions for simulation calculation were as follows: 50 000 Cu atoms were placed in a cubic box and then the system was run under periodic boundary conditions. The interacting interatomic potential adopted here is the quantum Sutton-Chen (Q-SC) many-body potentials[11–12], and the total energy of the system is obtained from the following equation:

$$U_{\text{tot}} = \sum_i U_i = \sum_i \left[\frac{1}{2} \sum_{j \neq i} D_{ij} V(r_{ij}) - C_i D_{ii} \rho_i^{1/2} \right] \quad (1)$$

where r_{ij} is the distance between atoms i and j , $V(r_{ij})$ is a pair of repulsive potential between atoms i and j (arising primarily from Pauli repulsion between the core electrons), i.e.

$$V(r_{ij}) = \left(\frac{\alpha_{ij}}{r_{ij}} \right)^n \quad (2)$$

While the metallic bonding is captured in ρ_i , a local energy density is associated with atom i and defined as

$$\rho_i = \sum_{j \neq i} \phi(r_{ij}) = \sum_{j \neq i} \left(\frac{\alpha_{ij}}{r_{ij}} \right)^n \quad (3)$$

where D sets the overall energy scale, c_i is a dimensionless parameter scaling the attractive term relative to the repulsive term, and α is an arbitrary length parameter leading to a dimensionless form for V and ρ .

Simulation parameters c_i , D , m , n and α are listed in Table 1. This potential was cut off at 22.0 a.u (atomic units), and the time step chosen was 1.0×10^{-14} s. The simulation calculation was started at 1 773 K (the melting point of Cu is 1 356 K). Firstly, let the system run at the same temperature (1 773 K) to get an equilibrium state (the criterion is the energy of the system being in an equilibrium state). Secondly, the temperature was decreased to some given temperatures from 1 673 to 173 K, the interval of two temperature points was 100 K, and let the system run 20 time steps at each given temperature to measure the structural configurations of this system, i. e., the space coordinates of each atom were recorded. Finally, the bond-types and their indexes between related atoms were detected by means of the index method of Honeycutt-Andersen (HA)[13], and the structural configurations of various clusters formed were described by the cluster-type index method(CTIM)[4]. Analyzing and comparing these results, we can get a clear physical picture on the microstructure transitions in the system from liquid state to amorphous state during rapid solidification processes.

Table 1 Parameters for Quantum Sutton-Chen(Q-SC) many-body potential used in this work[11–12]

D/meV	c	m	n	$\alpha/\text{\AA}$
5.792 1	84.843	5	10	3.603 0

3 Simulation results and analyses

3.1 Pair distribution function(PDF)

First of all, we inspect the pair distribution function $g(r)$ of the system obtained from the simulation, and find that it is consistent very well with the experimental results given by WASEDA[14], as shown in Fig.1. From

Fig.1, it can be seen that the Q-SC many-body potential function adopted here is successful in reflecting the objective physical nature of the system. In addition, from Fig.2, it can be seen that the first-peak gradually becomes higher and sharper with the temperature decreasing. When temperature drops to the range of 773–673 K, the second-peak of $g(r)$ begins to split. Finally, it entirely splits into two small peaks with a higher front sub-peak and a lower behind one, which is just one of the important characteristics of amorphous structures. This illuminates that the amorphous transition temperature of liquid metal Cu is about 673 K at the cooling rate of 1.0×10^{14} K/s.

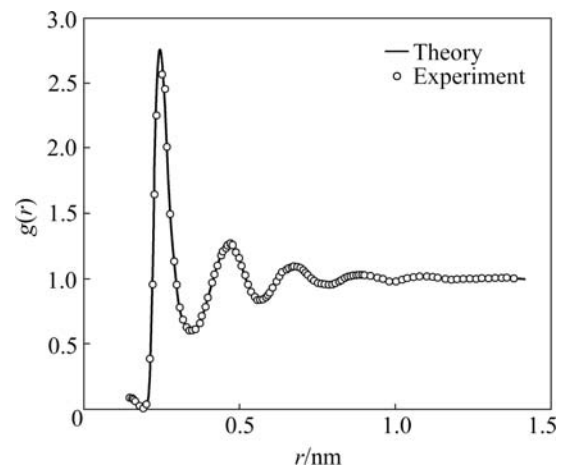


Fig.1 Pair distribution function $g(r)$ of liquid metal Cu at 1 573 K

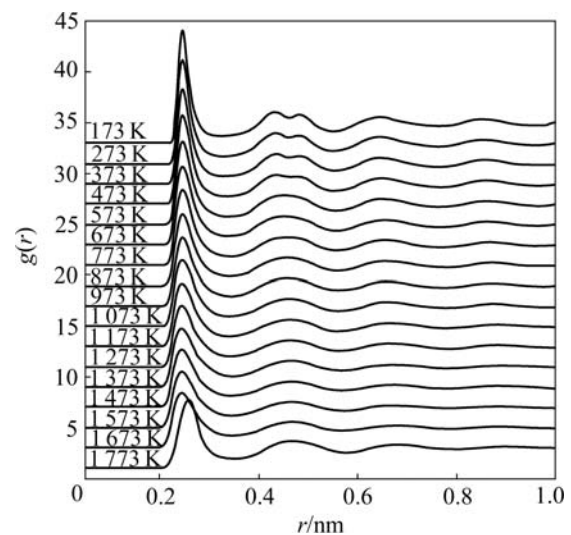


Fig.2 Relationships of pair distribution function $g(r)$ of liquid metal Cu with different temperatures

In order to further confirm the glass transition temperature T_g , we give the relationship between the Wendt-Abraham ratio (g_{\min}/g_{\max}) and temperature, as shown in Fig.3. The glass transition temperature T_g for the system is located at the intersection of liquid and

glass state[15]. According to Fig.3, T_g is approximately 673 K in our simulation, which agrees with the result of pair distribution function.

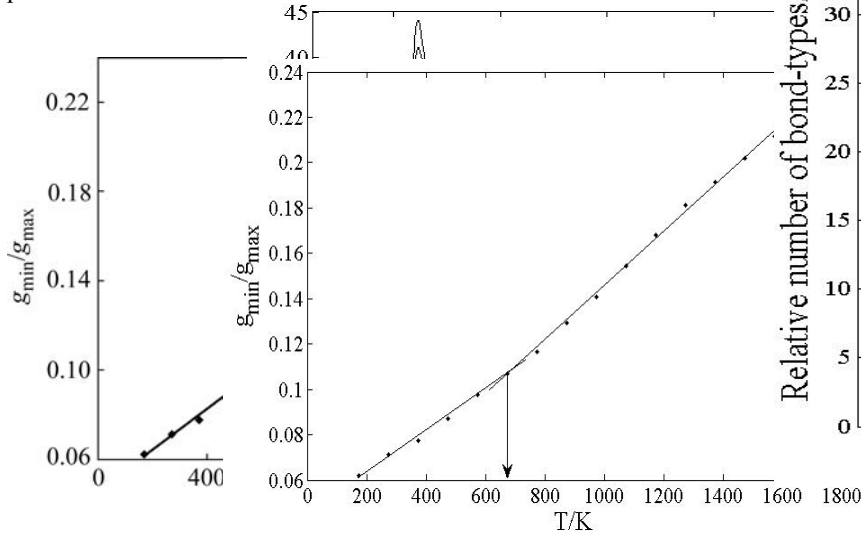


Fig.3 Relationship between g_{\min}/g_{\max} of liquid Cu and temperature

3.2 Bond-type analysis

In order to understand in depth the microstructural configurations of the system, it is not sufficient to analyze only the pair distribution function $g(r)$, and the bonding relationships between each atom with its neighbor atoms are also necessary to be known. Using method of HA bond-type indices, it is convenient to analyze geometric characteristics of atomic short-range arrangement formed in the system, and it is also the important way to analyze and study the microstructure characteristics of disorder system for liquid and amorphous states.

Method of HA bond-type indices[13] uses four integers i, j, k and l , to describe the structure of a pair of atoms under consideration. The first integer i is 1 if the pair is bonded and 2 otherwise. The second integer j represents the number of near neighbors shared by the pair of atoms. The third integer k denotes the number of bonds among the shared neighbors. However, it is not uniquely confirmed for some structural configurations by using i, j and k , so it is necessary to induce the fourth integer l to distinguish the pair atoms. Different bond types exist in various liquids, amorphous states and crystal structures. For example, the 1551, 1541 and 1431 bond types exist relatively numerous in typical liquid or amorphous states. The 1421 bond type represents the fcc-like local structure. The 1441 and 1661 bond types characterize the bcc-like local structure. The 1421 and 1422 bond types are found abundantly in hcp crystal structure. In this simulation, the relative bonding numbers obtained at various temperatures are shown in Fig.4. The following results can be obtained.

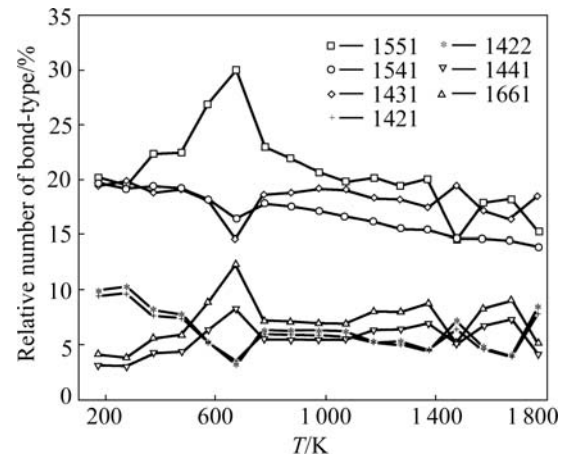
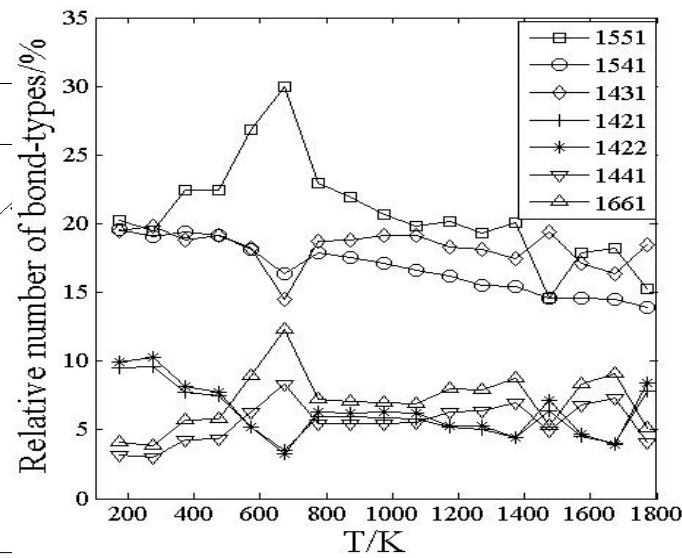


Fig.4 Relationships between relative numbers of seven main bond-types and temperature

1) The relative numbers of 1551, 1541 and 1431 bond-types, related to liquid and amorphous structures, are always in predominant position during the whole cooling processes. The three bond-types respectively occupy 15.3%, 13.89% and 18.49% of all bond-types at 1 773 K, and their sum amounts to 47.68% of the total number of bond types. When the temperature decreases to 173 K, the sum of them is 59.26%. Notably, the relative number of the 1551 bond type is up to its maximum of 30.01% at 673 K, and almost increases to be double of that at 1773 K. This shows that 1551 bond type plays an important role in the forming processes of amorphous structures.

2) The relative numbers of 1421 and 1422 bond-types related to fcc and hcp structures are 7.78% and 8.43 % at 1 773 K respectively. Moreover, they increase slowly with decreasing temperature, being 9.54% and 9.93% at 173 K, respectively.

3) The relative numbers of 1661 and 1441 bond types, related to bcc structure, decrease slowly with the

decrease of temperature, from 5.08% and 4.12% at 1 773 K to 4.11% and 3.2% at 173 K. Meanwhile, it is found that the variation tendency of 1551, 1441 and 1661 bond-types is almost the same during the cooling process. That is to say, all the amounts of 1551, 1441 and 1661 bond-types increase or decrease at the same range of temperature. This reflects that the variation of the symmetric configurations in the system is related synchronously to each other.

4) Notably, all the bond types change abruptly at 673 K. This shows that the phase transition of the system occurs at 673 K. Namely, the glass transition temperature of liquid metal Cu is about 673 K in this system.

3.3 Cluster-type analysis

For the disorder systems of liquid and amorphous states, the specific kinds and numbers of bond-types will form various clusters. In order to clearly express the structural characteristics, we adopt a new cluster-type index method(CTIM) to describe some important kinds of clusters. This method is based on the work of QI and WANG[16], who have successfully described the Frank-Kasper(FK) polyhedron, the Bernal polyhedron and other defective polyhedron. The CTIM also adopts four integers to express a basic cluster in turn as follows. The first integer represents the number of surrounding atoms, which form a cluster along with a central atom. The second, third and fourth integers represent the numbers of 1441, 1551 and 1661 bond-types formed by the surrounding atoms with the central atom, respectively. For example, (12 0 12 0) expresses an icosahedron cluster that is composed of 13 atoms (one is the central atom, the coordination number $Z=12$) connected with only twelve 1551 bond-types; (13 1 10 2) expresses the defective polyhedron cluster composed of 14 atoms (coordination number $Z=13$) connected with one 1441, ten 1551 and two 1661 bond-types respectively, as shown in Figs.5(a) and (b).

In order to more clearly express the physical picture of cluster structures, we further define the two concepts: a basic cluster and a polyhedron here[17]. A basic cluster is the smallest cluster composed of a central atom along with surrounding neighbor atoms, namely, each basic

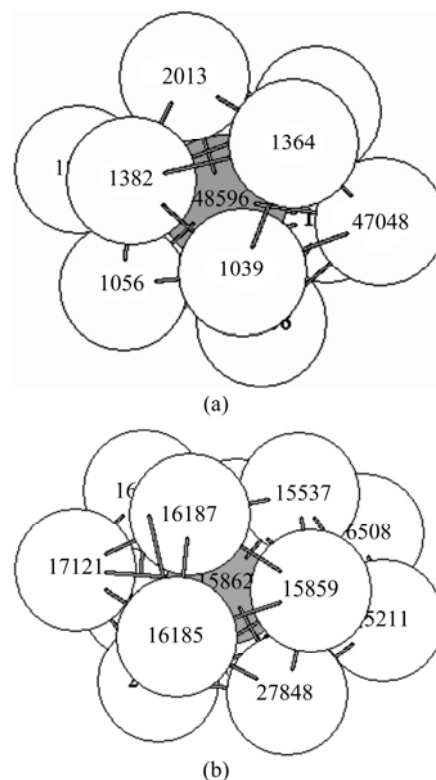
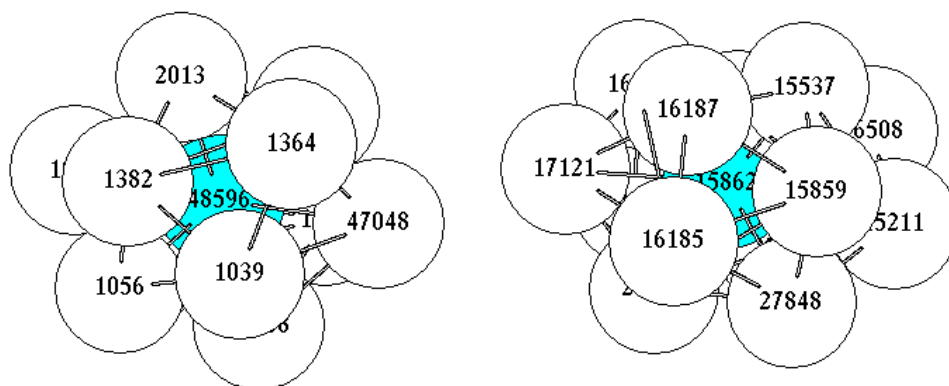


Fig.5 Schematic diagrams of icosahedron and defective polyhedron at 173 K: (a) Icosahedron (12 0 12 0) with centre atom numbered as 48 596; (b) Defective polyhedron (13 1 10 2) with centre atom of 15 862

cluster has one atom as the core of the cluster. A larger cluster can be formed by continuously growing up with a basic cluster as the core, or by combining several basic clusters. However, for a polyhedron structure, as usual, it is a hollow polyhedron with no central atom as the core. This is the essential distinction to basic cluster, such as well-known Bernal polyhedron. However, sometimes, if a basic cluster is named by the shape of the polyhedron composed of its surrounding neighbor atoms, the name maybe rather imaginary, so it is also called as a certain polyhedron cluster, such as icosahedron cluster, Bernal polyhedron cluster, and so on.

According to the CTIM, for the present simulation, the statistical numbers of various types of basic clusters are obtained, as listed in Table 2. It can be clearly seen that:

- 1) The basic clusters in the system can be classified by the number of surrounding atoms and divided into five sections according to



the number of surrounding neighbors of 12, 13, 14, 15 and 16 atoms, respectively. In the five sections, the numbers of basic clusters composed of 12, 13 and 14 neighbor atoms play a dominant role. However, the total numbers of basic clusters, which once appear during whole solidification processes, consisting of 13 surroundings neighbor atoms, are the largest (highly up to 7 163) among the five sections. This shows that in the system the basic cluster composed of 13 neighbor atoms is the most favorable to be formed, and that composed of 14 atoms (6 194) and 12 atoms (5 542) neighbor atoms is in the second and the third place in turn. However, among all the basic clusters, the number of icosahedral cluster (12 0 12 0) is the most one during the whole process of rapid solidification.

2) Among twenty-one cluster-types of five sections (here the clusters that appear more than twenty times during the whole solidification process are listed only), the number of 1441 bond-type in clusters appears as 0, 1, 2, 3, 4 and 5 (being an ascending integer series); the number of 1551 bond-type as 12, 10, 8, 6 and 4 (being a descending even integer series); and the number of 1661 bond-type as 0, 1, 2, 3, 4, 5, 6 and 7 (being an ascending integer series). The basic clusters, which are formed by three bond-types with proper ratios and numbers, have lower energy and more stable structure (such as the basic clusters being expressed in turn as (12 0 12 0), (13 1 10 2), (14 2 8 4), (14 1 10 3) and (13 3 6 4). They indeed have this sequence according to the average energy of each bond-type), so they have the strongest ability of formation and become the major clusters in the system.

3) The number of icosahedra expressed by (12 0 12 0) increases sharply from 86 at 1 773 K to 300 at 173 K, and their relative numbers to the total number of clusters are occupied from 13.3% to 42.6%, respectively.

Table 2 Relationships of numbers of various cluster-types with different temperatures

Type of cluster	Temperature/K																
	1 773	1 673	1 573	1 473	1 373	1 273	1 173	1 073	973	873	773	673	573	473	373	273	173
(12 0 12 0)	86	63	59	69	103	96	126	156	191	237	288	478	514	340	358	253	300
(12 2 8 2)	53	80	73	47	103	82	78	82	92	75	99	221	126	52	38	10	20
(12 3 6 3)	19	39	28	11	42	33	33	27	21	24	19	46	18	4	1	3	2
(12 4 4 4)	4	19	11	5	7	13	10	7	6	7	5	21	5	3	1	0	0
(13 1 10 2)	104	125	132	79	165	165	177	176	182	216	233	613	395	196	185	90	93
(13 2 8 3)	21	46	51	21	62	55	48	48	50	43	39	164	77	26	25	6	9
(13 3 6 4)	86	131	129	74	151	151	170	145	145	153	153	553	280	87	133	40	59
(13 4 4 5)	12	21	30	11	26	27	25	9	15	26	15	49	22	4	7	1	2
(13 5 2 6)	1	4	6	2	5	7	8	4	7	5	5	25	10	1	3	0	1
(14 0 12 2)	11	9	13	10	33	26	31	30	39	36	60	101	84	44	46	41	44
(14 1 10 3)	28	48	47	31	56	53	70	60	47	83	73	250	141	51	45	18	13
(14 2 8 4)	56	88	75	48	130	133	131	102	107	124	154	481	247	106	106	24	43
(14 3 6 5)	28	65	65	23	87	78	75	76	63	73	78	307	140	35	39	9	11
(14 4 4 6)	22	27	48	18	44	55	47	48	53	54	75	285	135	39	36	10	19
(15 0 12 3)	12	7	10	5	8	10	11	6	14	11	16	36	27	27	19	8	12
(15 1 10 4)	14	30	26	12	34	42	40	30	27	42	54	126	105	39	31	13	7
(15 2 8 5)	25	33	31	17	47	40	43	35	40	38	51	187	104	25	26	8	11
(15 3 6 6)	12	18	32	11	27	22	24	15	16	22	23	122	38	17	10	3	2
(15 4 4 7)	3	10	8	6	9	17	10	12	8	9	11	65	26	9	3	2	2
(16 1 10 5)	2	6	6	4	6	7	6	7	8	5	8	34	9	4	2	1	0
(16 2 8 6)	2	7	3	4	8	8	2	3	4	6	3	34	10	1	0	0	0
Total number of all clusters	647	954	936	525	1 229	1 184	1 211	1 118	1 162	1 319	1 501	4 318	2 566	1 136	1 142	636	705

Especially, while the temperature decreases to 573 K, the number of (12 0 12 0) cluster reaches the maximum 514. Therefore, the icosahedral clusters play an important role in the microstructure transition during the rapid cooling processes of liquid metal copper. However, the relative numbers of other important clusters, such as the basic clusters expressed as (13 1 10 2), (14 1 10 3), (15 1 10 4), (12 2 8 2), (14 2 8 4) and (13 3 6 4), are also occupied the maximum at temperature of 673 K. Fig.6 shows the relationship of the total number of basic clusters with temperature. It can be found that the total number of clusters increases slowly with decreasing temperature above 773 K. But when the temperature drops to 673 K, the total number increases abruptly (reaching the maximum of 4 318), and subsequently decrease suddenly. This also shows that the phase transformation takes place in the system from liquid to amorphous state at this temperature. This result is consistent with that of the bond-type analysis mentioned above.

4) Notably, from Fig.6, it can be obviously seen that the total number of various clusters in the system decreases abruptly when temperature is below 673 K. In fact, the microstructure transition of liquid metal Cu during the solidification processes is more complicated. The basic clusters described by CTIM are limited to

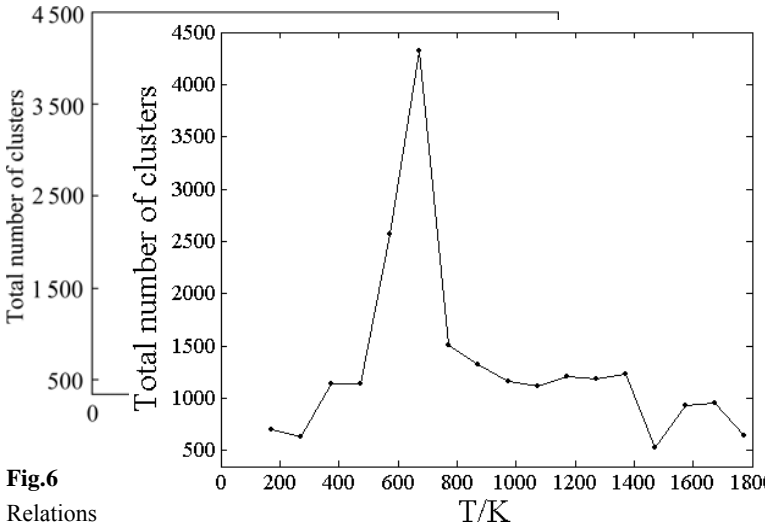


Fig.6
Relations
hip between total number of clusters and temperature

those formed only with 1441, 1551 and 1661 bond-types in the system, and other basic clusters formed with other bond-types, such as 1311, 1321, 1421, 1422, 1431 and 1541, have not be described by CTIM until now, so the result shown in Fig. 6 is rather simple. However, it is interesting that the three bond types 1441, 1551 and 1661 just decrease abruptly below 673 K in Fig.4, and this is just consistent with the analyzing results above.

5) The Frank-Kasper(FK) polyhedron expressed as (14 0 12 2) and (15 0 12 3) is also contained with a certain amount in the system.

3.4 Mean square displacement(MSD)

Fig.7 shows the relationship between the mean square displacement(MSD) and temperature in the cooling process. It can be seen that the slope of MSD curve drops gradually as the temperature lowers. This shows that with the temperature decreasing, the order degree in the system is enhanced gradually and the fluidity of the system is weakened. While temperature is decreased to below 673 K, the slope of MSD curve is near to zero, this means that the system has no fluidity and begins to solidify below this temperature, so the temperature is also corresponded to the glass transition temperature, and consistent with analysis mentioned above.

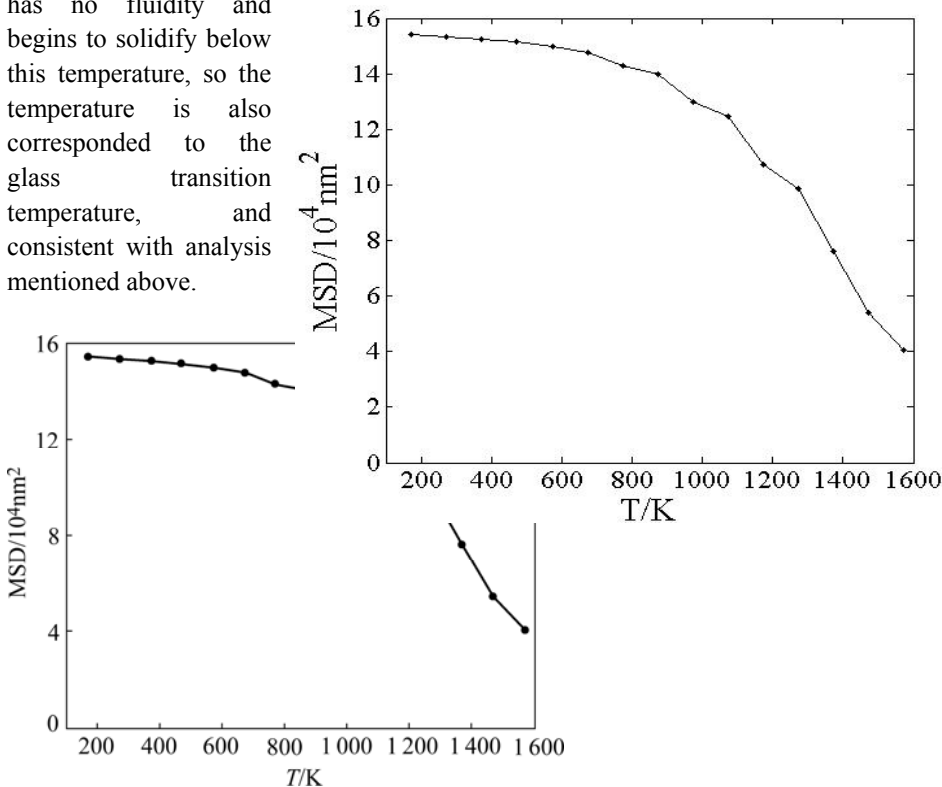
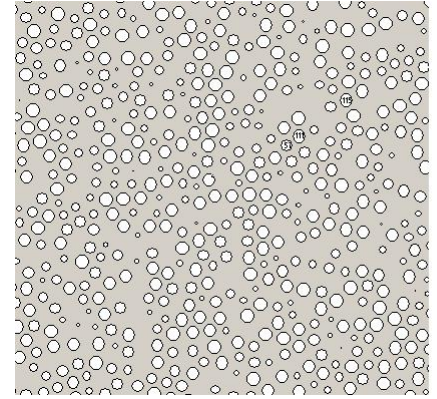
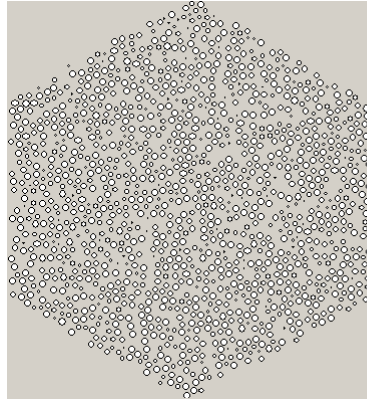


Fig.7 Relationships between mean square displacement(MSD) and temperature during cooling process

3.5 Visualization analysis

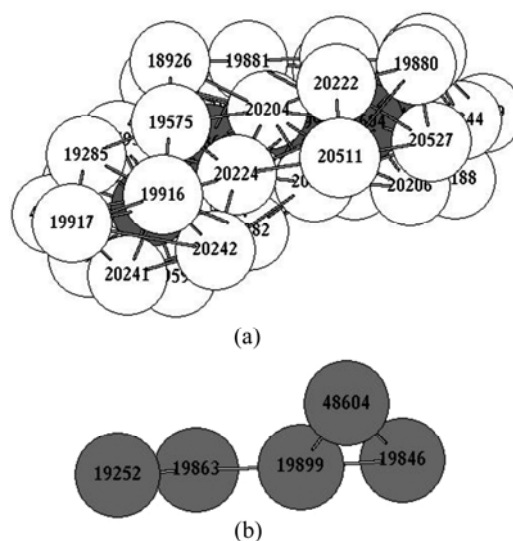
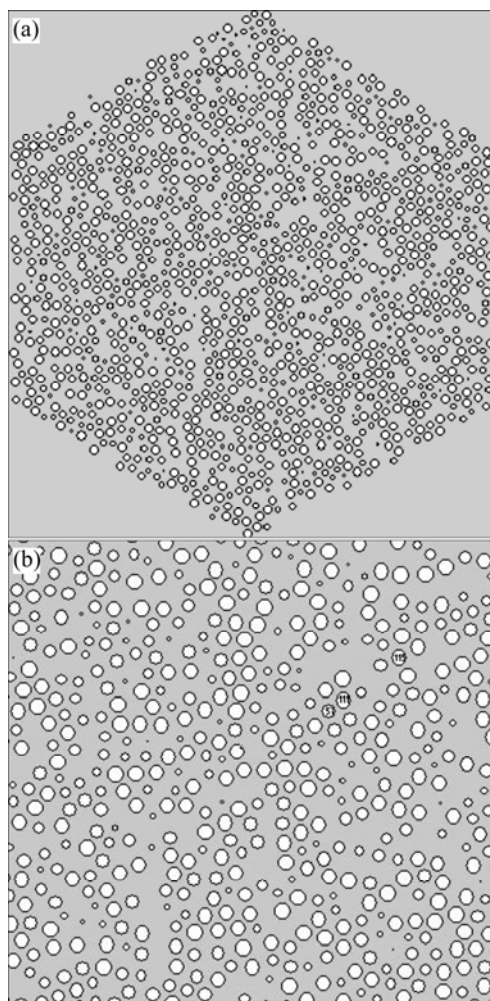
For convenience of discussion, the schematic diagram of the cross section of 50 000 Cu atoms system at 173 K is shown in Figs.8(a) and (b), with the whole (111) cross section and a part of (111) cross section ($\times 2$ times), respectively. It can be clearly seen that the system is formed into amorphous structure from liquid state by rapid cooling, and composed of two types of areas: the relative dense area and sparse area. In the dense area, there are cluster structures with different

sizes, in which the atoms are arranged according to a certain rule and possess short-range order characteristics;



and in the sparse area, the atoms are distributed randomly. From the viewpoint of the whole system, the amorphous structures indeed possess characteristic of long-range disorder and short-range order.

In addition, there exists a nano-cluster consisting of 41 atoms within 5 basic clusters as shown in Fig.9. The central atoms of basic clusters are expressed by the black spheres. It can be clearly seen that the nano-cluster is



linked by two single basic clusters and one middle clusters with three basic clusters shaped as a triangle. However, this is the essential distinction of the nano-cluster configurations to those obtained by gaseous deposition and ionic spray. The latter is the nano-level crystal clusters formed by octahedron-shells configuration accumulated with an atom as the center[18].

each other, such as 19252, 19863 central atoms in Fig.9(b), so the two basic clusters are connected rather tight. However, as the central atoms linked by multi-bonds are near neighbor with each other, such as 19899, 19846 and 48604 central atoms, the three basic clusters will be connected more tightly. That is to say, the more the central atoms of the basic clusters linked by multi-bonds, the more stable the nano-cluster during solidification processes.

4 Conclusions

1) The Q-SC many-body potential function adopted here is successful in reflecting the objective physical nature of forming amorphous microstructures. During the whole rapid cooling process of liquid metal system consisting of 50 000 Cu atoms, the three bond-types of 1551, 1541 and 1431, and the icosahedron and other basic clusters of (12 0 12 0), (12 2 8 2), (13 1 10 2), (13 3 6 4), (14 1 10 3), (14 2 8 4) and (15 1 10 4), play a critical and leading role in the microstructure transitions.

2) At the cooling rate of 1.0×10^{14} K/s, the glass transition temperature is 673 K. At 673 K, the sum of all various clusters reaches the most numbers, namely, the microstructure configurations of the system have an important transition.

3) The nano-clusters formed in the system are composed of some basic clusters or middle clusters by connecting to each other, and each middle cluster also consists of some basic clusters. This is the essential distinction of the nano-cluster configurations to those obtained by gaseous deposition and ionic spray. The more the central atoms of the basic clusters linked by multi-bonds, the more stable the nano-cluster during solidification processes.

References

- [1] LIU R S, DONG K J, TIAN Z A, LIU H R, PENG P, YU A B. Formation and magic number characteristics of clusters formed during solidification processes [J]. *J Phys: Condens Matter*, 2007, 19: 196103.
- [2] CHEN F F, ZHANG H F, QIN F X, HU Z Q. Molecular dynamics study of atomic transport properties in rapidly cooling liquid copper [J]. *J Chem Phys*, 2004, 120(4):1826–1831.
- [3] LI H, WANG G H, BIAN X F, DING F. Local cluster formation in a cobalt melt during the cooling process [J]. *Phys Rev B*, 2003, 65: 035411.
- [4] DONG K J, LIU R S, YU A B, ZOU R P, LI J Y. Simulation study of the evolution mechanisms of clusters in a large-scale liquid Al system during rapid cooling processes [J]. *J Phys: Condens Matter*, 2003, 15: 743–753.
- [5] CHEN K Y, LIU H B, LI X P, HAN Q Y, HU Z Q. Molecular dynamics simulation of local structure of aluminium and copper in supercooled liquid and solid state by using EAM [J]. *J Phys: Condens Matter*, 1995, 7: 2379–2394.
- [6] YUE Q, TAHIR C, YOSHITAKES K, GODDARD W A. Molecular-dynamics simulation of glass formation and crystallization in binary liquid metals: Cu-Ag and Cu-Ni [J]. *Phys Rev B*, 1999, 59(5): 3527–3533.
- [7] WANG L, BIAN X F AND LI H. Liquid-solid transition and crystal growth of metal Cu by molecular dynamics simulation [J]. *Acta Phys Chim Sin*, 2000, 16(9): 825–829. (in Chinese)
- [8] ZHANG T, ZHANG X R, GUAN L, QI Y H, XU C Y. The simulation of metal Cu in the melting and solidification process [J]. *Acta Metal Sin*, 2004, 40(3): 251–256. (in Chinese)
- [9] LIU C S, XIA J C, ZHU Z G, SUN D Y. The cooling rate dependence of crystallization for liquid copper: A molecular dynamics study [J]. *J Chem Phys*, 2001, 114(17): 7506–7512.
- [10] DONG K J, LIU R S, ZHENG C X, LIU H R, PENG P, LU X Y. Parallel algorithm of solidification process simulation for large-sized system of liquid metal atoms [J]. *Trans Nonferrous Met Soc China*, 2003, 13(4): 824–829.
- [11] SUTTON A P, CHEN J. Long-range Finnis-Sinclair potentials [J]. *Pilos Mag Lett*, 1990, 61(3): 139–146.
- [12] DOYE J P K, WALES D J. Global minima for transition metal clusters described by Sutton-Chen potentials [J]. *New J Chem*, 1998, 22: 733–744.
- [13] HONEYCUTT J D, ANDERSEN H C. Molecular-dynamics study of melting and freezing of small Lennard-Jones clusters [J]. *J Chem Phys*, 1987, 91: 4950–4963.
- [14] WASEDA Y. The structure of non-crystalline materials [M]. New York: Mcraw-Hill, 1981: 270.
- [15] WENDT H R, ABRAHAM F F. Empirical criterion for the glass transition region based on Monte Carlo simulations [J]. *Phys Rev Lett*, 1978, 41: 1244–1246.
- [16] QI W D, WANG S. Icosahedral order and defects in metallic liquid and glasses [J]. *Phys Rev B*, 1991, 44: 884–887.
- [17] LIU R S, DONG K J, LIU F X, ZHENG C X, LIU H R, LI J Y. Formation and evolution mechanisms of large-clusters during rapid solidification process of liquid metal Al [J]. *Science in China Ser G*, 2005, 48(1): 101–112.
- [18] MARTIN T P, NAHER U, SCHABER H. Evidence for octahedral shell structure in aluminum clusters [J]. *Chem Phys Lett*, 1992, 199(5): 470–474.

(Edited by LI Xiang-qun)